Supporting Information

Laser Processing of Li-doped Mesoporous TiO_2 for Ambient-processed Mesoscopic Perovskite Solar Cells

Hongbo Mo, [ab1] Qian Chen, [a1]* Dong Wang,[a] Wei Guo,[b] Dongxu Cheng,[b] Yang Sha,[a] Muhamad Z. Mokhtar,[a] Zhenyu Jia,[a] Janet Jacobs,[b] Andrew G Thomas,[acd] Lin Li,[b] Zhu Liu,[ae]* and Richard J Curry[cd]*

[a] Department of Materials, The University of Manchester, Oxford Road, Manchester, M13 9PL, UK

[b] Laser Processing Research Center, Department of Mechanical, Aerospace and Civil Engineering, The University of Manchester, Oxford Road, Manchester, M13 9PL, UK

[c] Photon Science Institute, Department of Electrical and Electronic Engineering, The University of Manchester, Oxford Road, Manchester, M13 9PL, UK

[d] Henry Royce Institute, The University of Manchester, Oxford Road, Manchester M13 9PL, UK

[e] Research Centre for Laser Extreme Manufacturing, Ningbo Institute of Materials Engineering and Technology, Chinese Academy of Science, Ningbo, China.

[*] Corresponding authors: qian.chen-2@manchester.ac.uk; liuzhu@nimte.ac.cn; richard.curry@manchester.ac.uk

[1] These authors have contributed equally to this work.

Keywords

Laser treatment, mesoporous TiO_2, doped-TiO_2, Ambient-processed, Perovskite solar cells

Figure S1 Humidity meter showing relative humidity 72.8% during the fabrication of the PSCs.

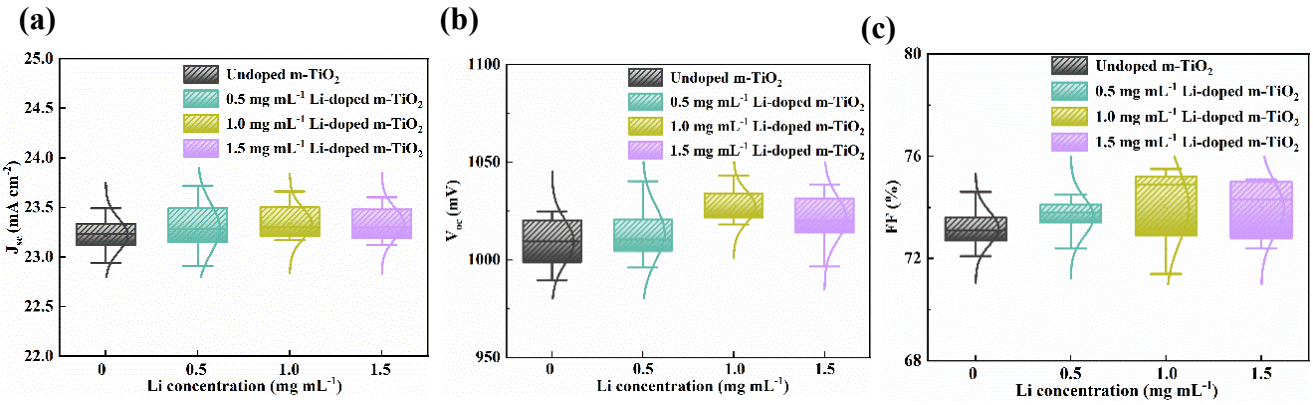

Figure S2 (a) J_{SC} and (b) V_{OC} (c) FF distribution for the PSCs based on the m-TiO_2 with various Li doping concentration.

(a)

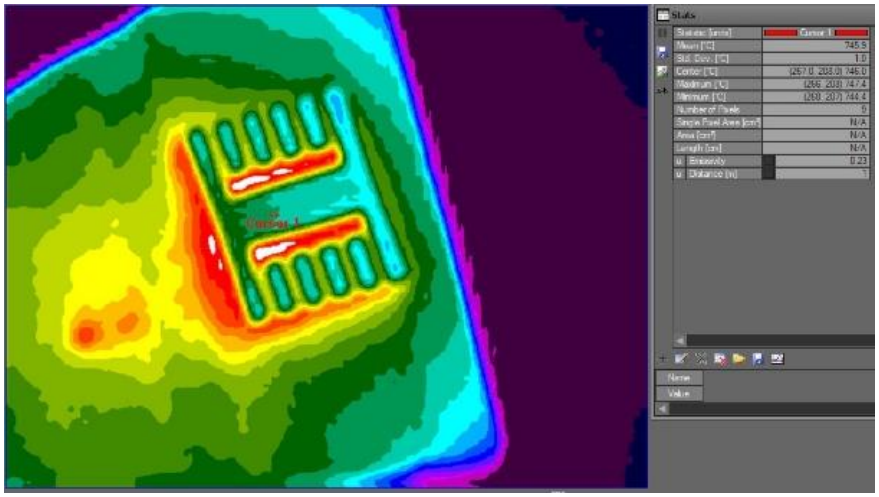

(b)

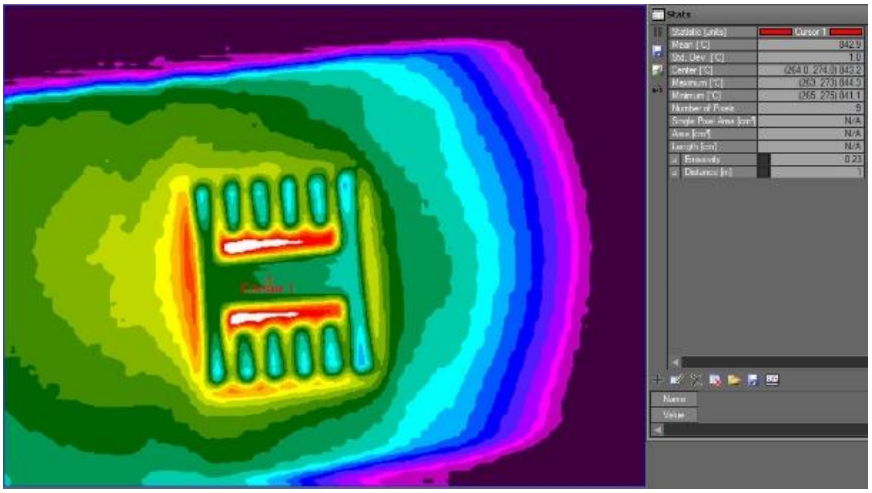

(c)

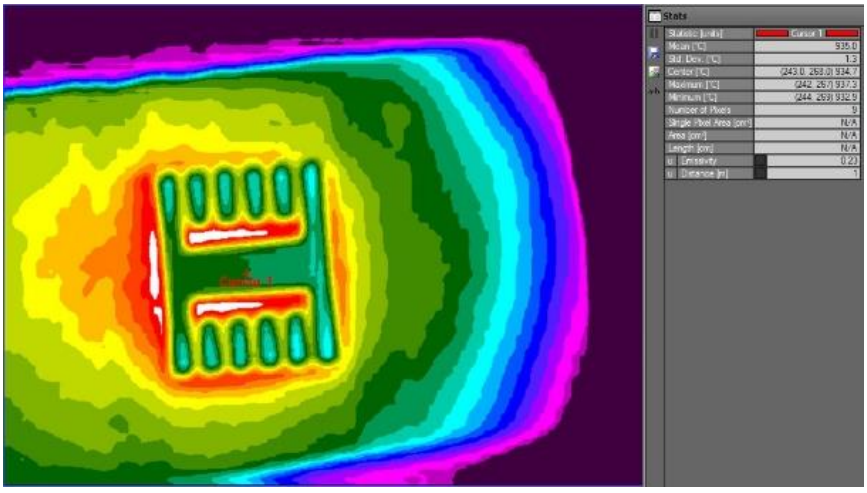

Figure S3 Thermal profiles of the laser-treated Li-doped m-TiO_2 on the ITO-glass with highest treatment temperatures of (a) 700-750, (b) 800-850, and (c) 900-950 °C.

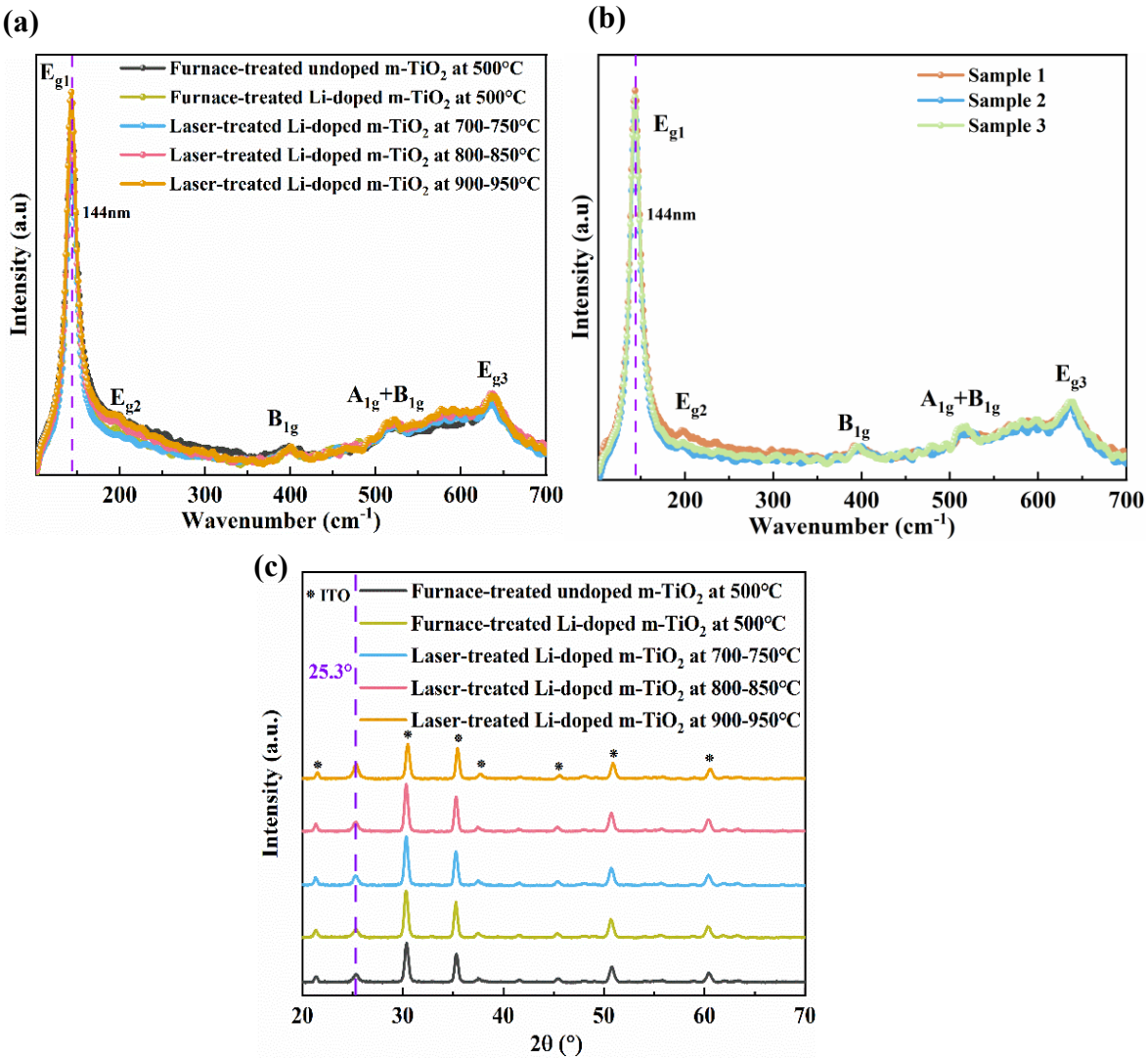

Figure S4 (a) Raman spectra of the furnace-treated undoped m-TiO_2, furnace- and laser-treated Li-doped m-TiO_2 films, (b) Raman Spectra for 3 different samples with condition of laser-treated Li-doped m-TiO_2 films at 850°C. and (c) XRD patterns of the furnace-treated undoped m-TiO_2, furnace- and laser-treated Li-doped m-TiO_2 films.

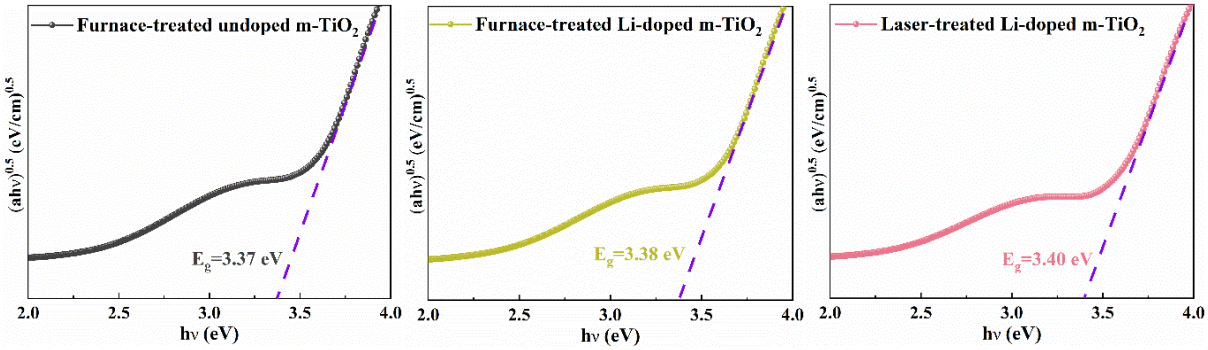

Figure S5 Tauc plots for (a) furnace-treated undoped m-TiO_2, (b) furnace-treated Li-doped m-TiO_2 and (c) laser-treated Li-doped m-TiO_2 (800-850 °C).

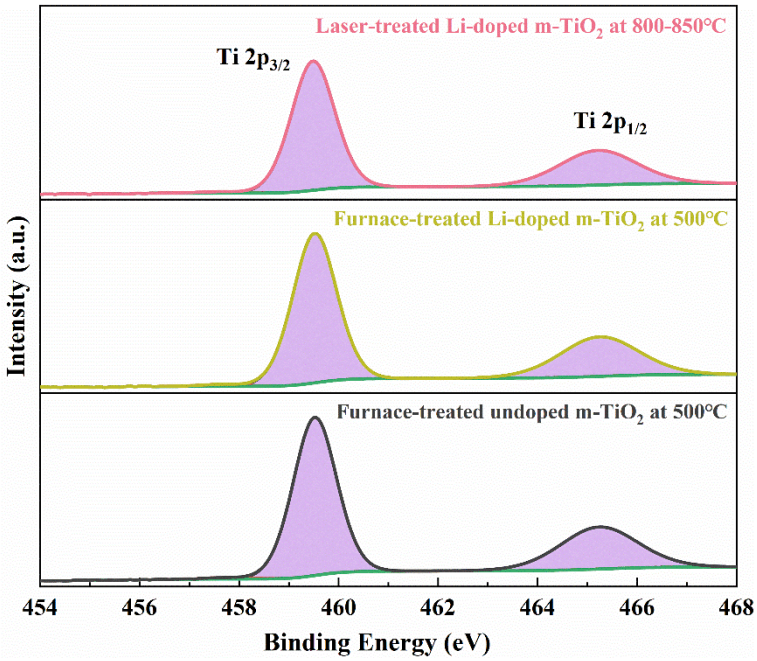

Figure S6 XPS high resolution profile of Ti 2p for the furnace-treated undoped m-TiO_2, Li-doped m-TiO_2 and laser-treated Li-doped m-TiO_2 films (800-850 °C).

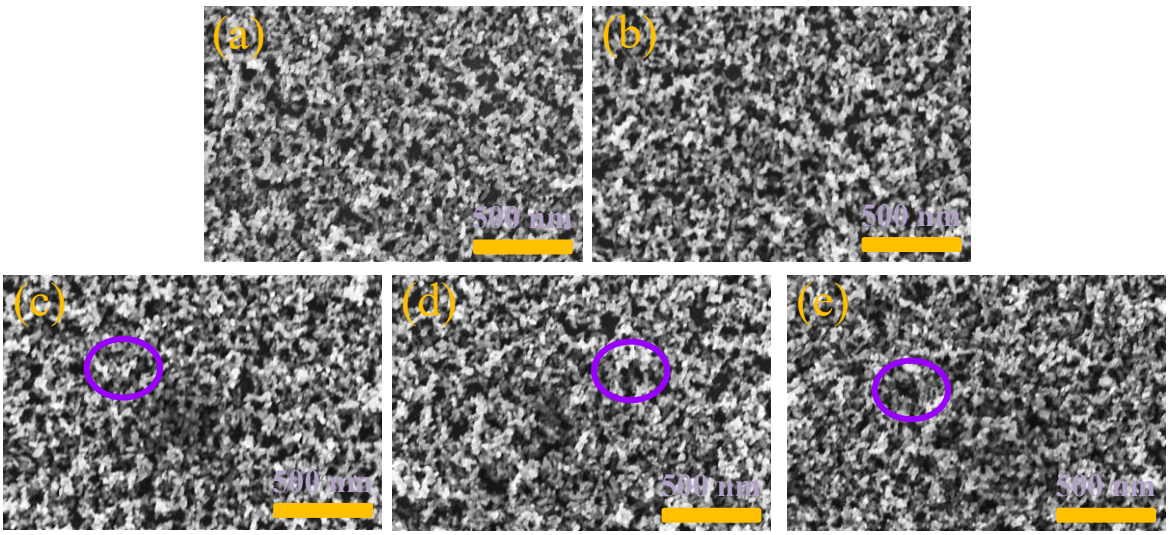

Figure S7 Top view SEM images for (a) furnace-treated undoped m-TiO_2 film, (b) furnace-treated Li-doped m-TiO_2 film and laser-treated Li-doped m-TiO_2 films with the highest annealing temperature of (c) 700–750 ℃, (d) 800–850 ℃, (e) 900–950 ℃ (interconnected TiO_2 particles marked in purple circle, scale bar = 500 nm).

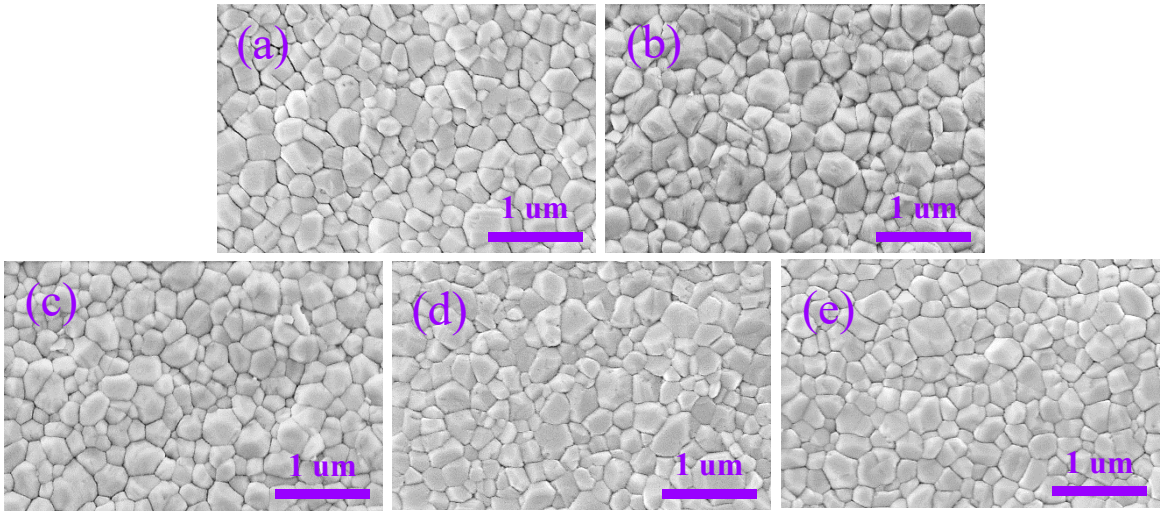

Figure S8 Top view SEM images for the perovskite film deposited on (a) furnace-treated undoped m-TiO_2 film, (b) furnace-treated Li-doped m-TiO_2 film and laser-treated Li-doped m-TiO_2 films with the highest processing temperature of (c) 700–750 ℃, (d) 800–850 ℃, (e) 900–950 ℃ (scale bar = 1 um).

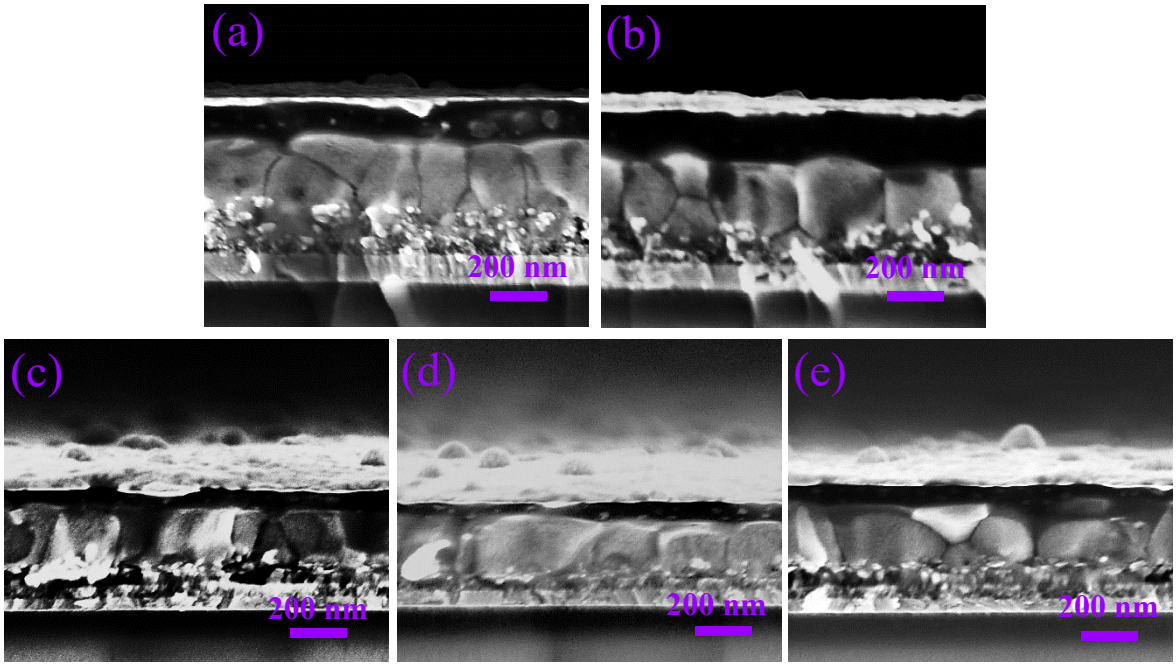

Figure S9 Cross-sectional SEM view for the PSCs based on the (a) furnace-treated undoped m-TiO_2 film, (b) furnace-treated Li-doped m-TiO_2 film and laser-treated Li-doped m-TiO_2 films with the highest processing temperature of (c) 700–750 ℃, (d) 800–850 ℃, (e) 900–950 ℃.

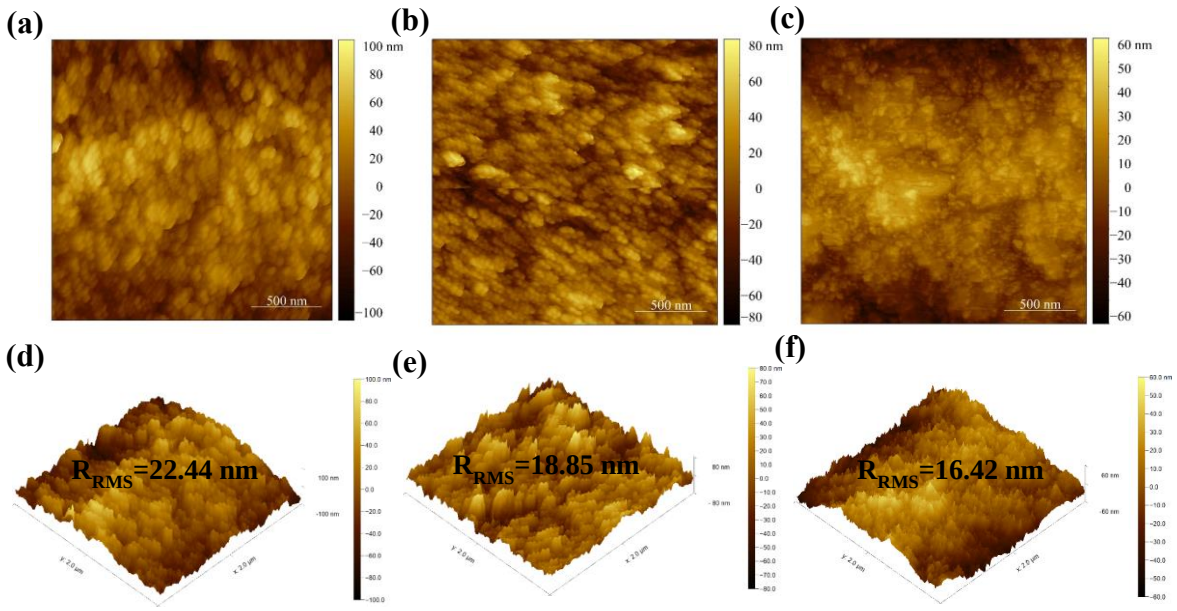

Figure S10 AFM topography for (a,d) furnace-treated undoped m-TiO_2, (b,e) furnace-treated Li-doped m-TiO_2 and (c,f) laser-treated Li-doped m-TiO_2 (800-850 °C).

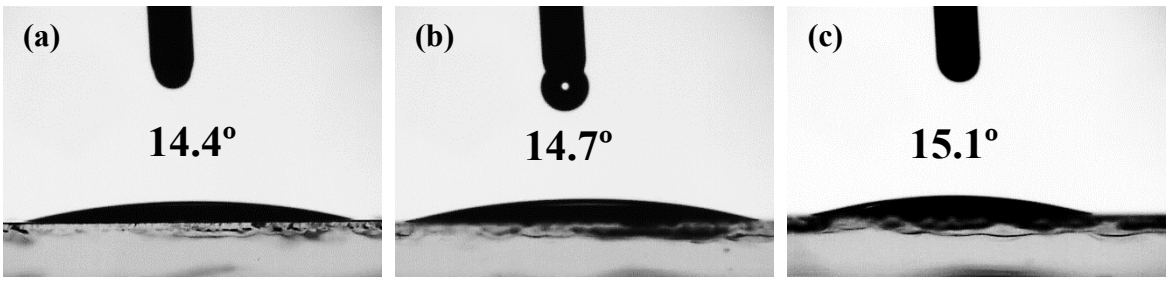

Figure S11 Water contact measurements for (a) furnace-treated undoped m-TiO_2, (b) furnace-treated Li-doped m-TiO_2 and (c) laser-treated Li-doped m-TiO_2 (800-850 °C).

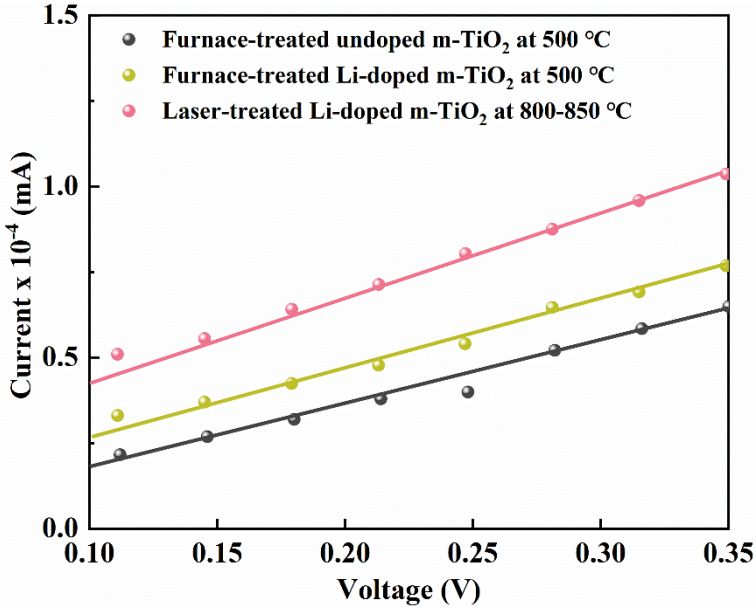

Figure S12 *I-V* curves ohmic region of the furnace-treated undoped m-TiO_2, Li-doped m-TiO_2 and laser-treated Li-doped m-TiO_2 films (800-850 °C).

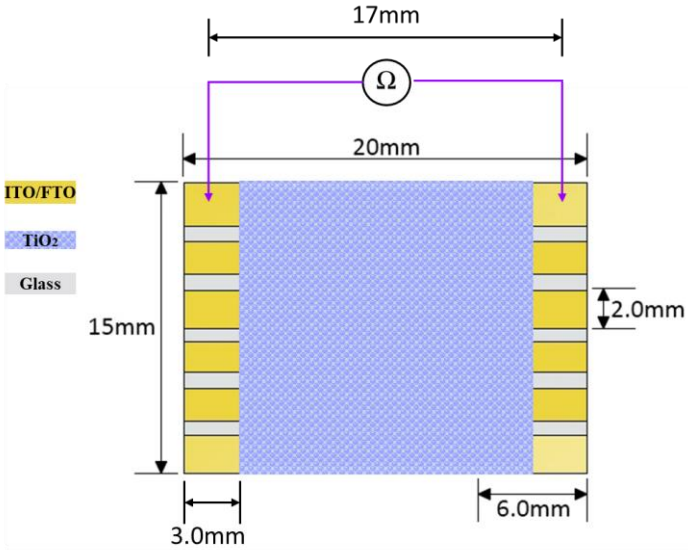

Figure S13 Schematic representation of the ITO/FTO resistance measurement by two-probe method with a measure distance of 17 mm between the two electrodes.

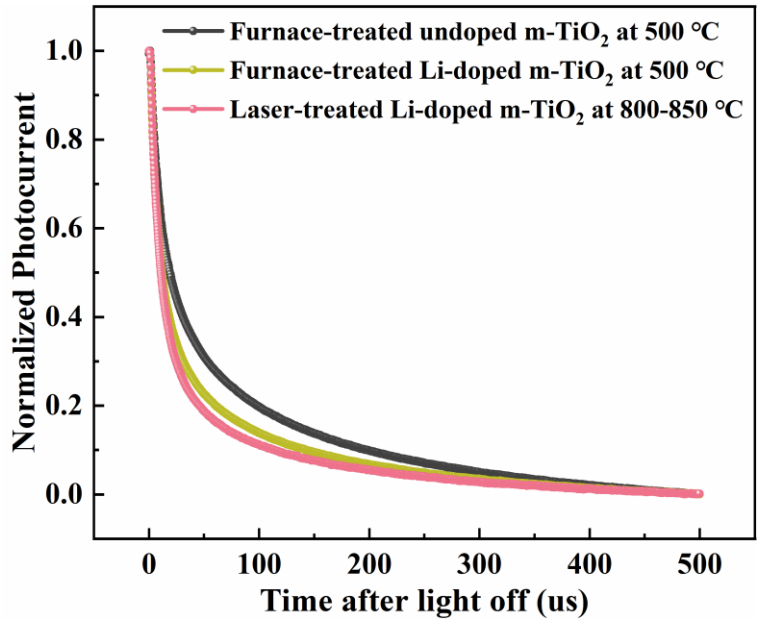

Figure S14 Transient photo-current decay of PSCs based on furnace-treated undoped m-TiO_2, Li-doped m-TiO_2 and laser-treated Li-doped m-TiO_2 films (800-850 ℃).

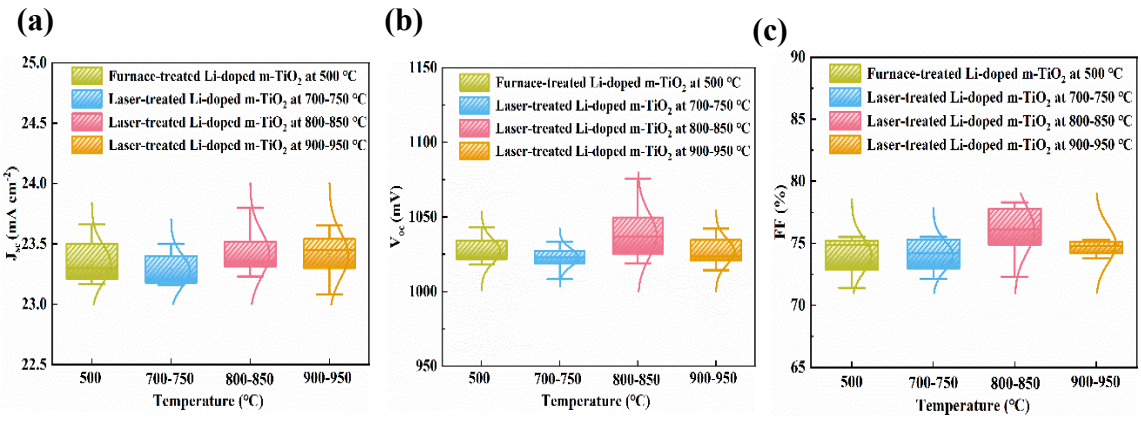

Figure S15 (a) J_{SC} and (b) V_{OC} (c) FF distribution for PSCs based on furnace-treated Li-doped m-TiO_2 and laser-treated Li-doped m-TiO_2 films.

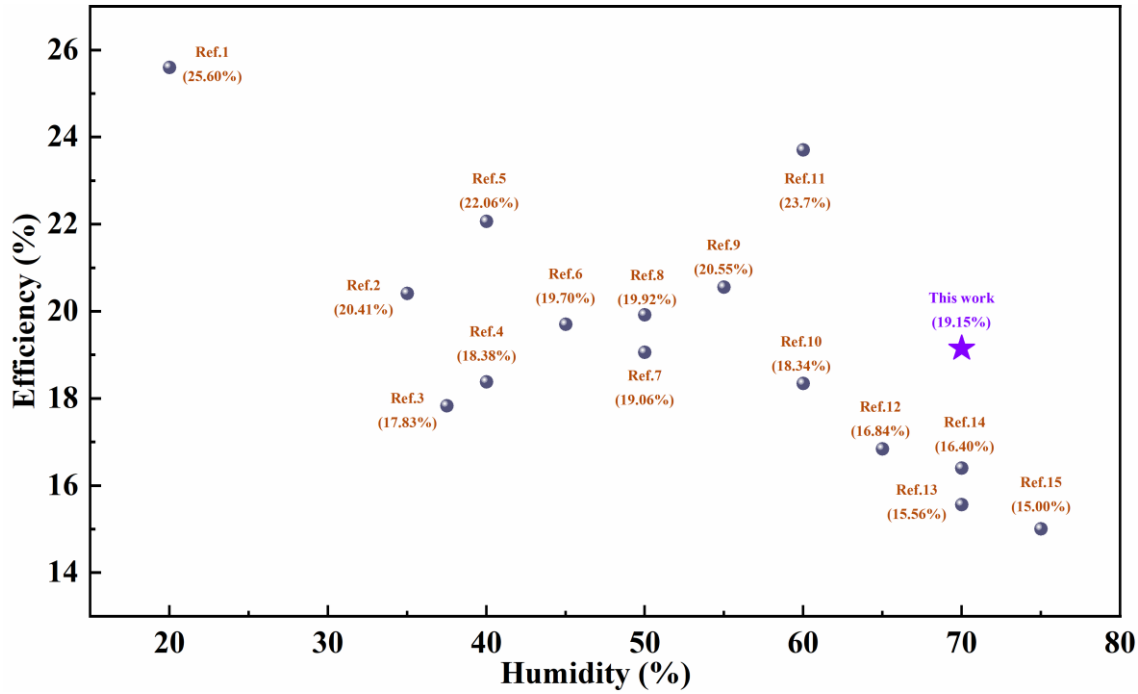

Figure S16 The summary of the state-of-the-art efficiencies for ambient processed PSCs under various humidity [1–15].

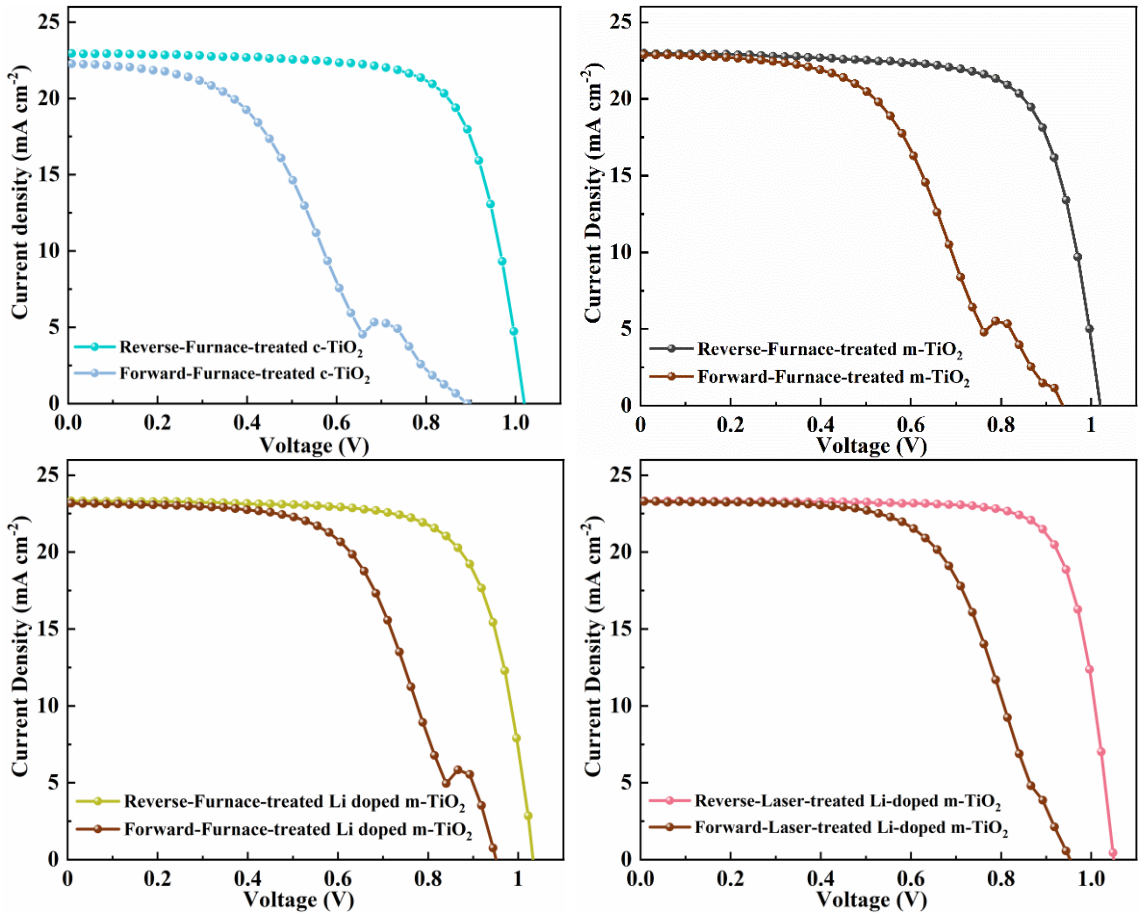

Figure S17 The *J-V* curves of PSCs measured in reverse and forward scan for (a) furnace-treated pure c-TiO_2. (b) furnace-treated pure m-TiO_2, (c) furnace-treated Li doped m-TiO_2, and (d) laser-treated Li-doped m-TiO_2.

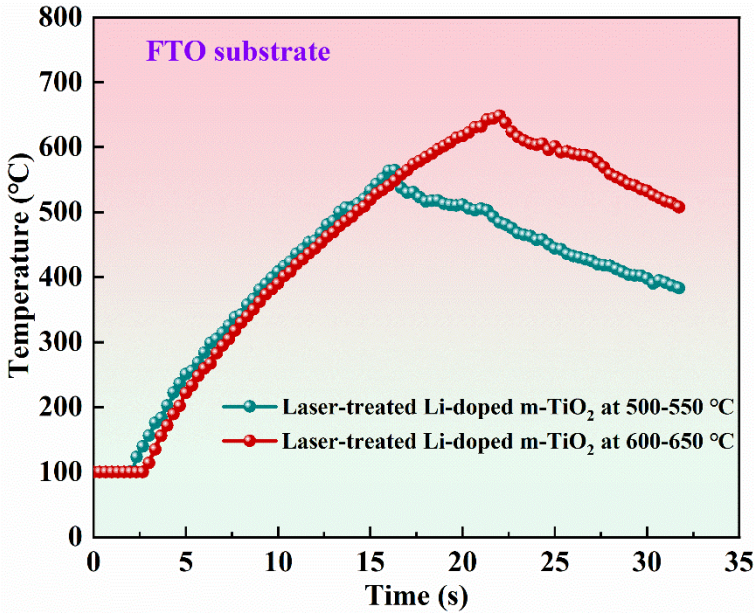

Figure S18 Temperature profiles of Li-doped m-TiO_2 films coated on FTO substrate during laser treatment with various laser parameters settings.

(a) **(b)**

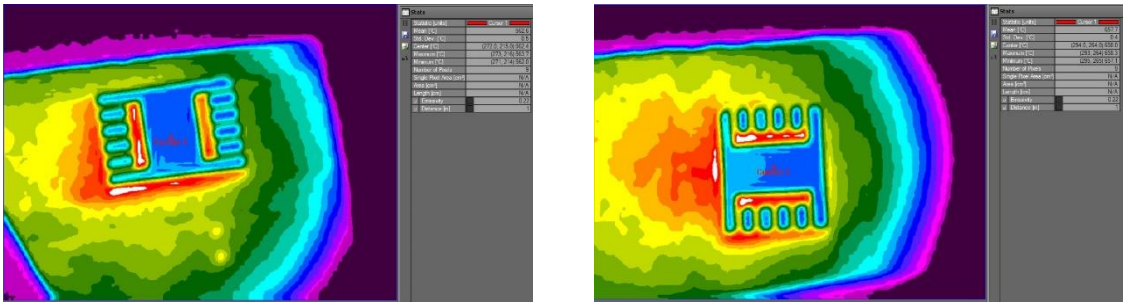

Figure S19 Thermal profiles of the laser-treated Li-doped m-TiO_2 on the FTO glass with peak treatment temperatures of (a) 500-550 and (b) 600-650 °C.

Table S1 Summary of photovoltaic parameters for the mesoporous PSCs with the furnace-treated undoped m-TiO_2 and Li-doped m-TiO_2 films.

Samples	V_{OC} (V)	J_{SC} (mA·cm^{-2})	FF (%)	Average PCE (%)	Champion PCE (%)
Undoped m-TiO_2	1.010±0.011	23.22±0.16	73.19±0.64	17.16±0.19	17.71
0.5 mg mL^{-1} Li-doped m-TiO_2	1.014±0.014	23.29±0.24	73.63±0.72	17.38±0.29	17.86
1.0 mg mL^{-1} Li-doped m-TiO_2	1.027±0.008	23.34±0.15	74.03±1.33	17.74±0.31	18.10
1.5 mg mL^{-1} Li-doped m-TiO_2	1.021±0.011	23.34±0.15	73.95±0.98	17.63±0.35	18.04

Table S2 Laser processing parameters for the fabrication of Li-doped TiO_2 films.

	Temperatures (Measured by thermal cameral)	Spot area (cm^2)	Ramp power density (W·cm^2)	Duration (s)	Soak power density (W·cm^2)	Duration (s)
Li-doped m-TiO_2/ITO	Laser-treated at 700-750 ºC	196	113	14	36	3
	Laser-treated at 800-850 ºC		113	18	36	3
	Laser-treated at 900-950 ºC		113	22	36	3
Li-doped m-TiO_2/FTO	Laser-treated at 500-550 ºC	196	113	14	36	3
	Laser-treated at 600-650 ºC		113	18	36	3

Table S3 Summary of XRD peak position, peak intensity, FWHM, and crystalline size calculated using Scherrer equation for the furnace-treated undoped m-TiO_2 and furnace- and laser-treated Li-doped m-TiO_2 films.

Conditions	Peak position 2θ (º)	FWHM (º)	Peak intensity	Crystal size (nm)
Furnace-treated undoped m-TiO_2 at 500 ºC	25.3	0.638	669	12.76
Furnace-treated Li-doped m-TiO_2 at 500 ºC	25.3	0.653	527	12.47
Laser-treated Li-doped m-TiO_2 at 700-750 ºC	25.3	0.726	517	11.21
Laser-treated Li-doped m-TiO_2 at 800-850 ºC	25.3	0.628	708	12.96
Laser-treated Li-doped m-TiO_2 at 900-950 ºC	25.3	0.617	784	13.20

Table S4 The Calculated details for the energy level of furnace-treated undoped m-TiO_2, Li-doped m-TiO_2 at 500ºC and laser-treated Li-doped TiO_2 at 800-850 ºC

Conditions	E_f (eV)	E_{onset} (eV)	E_g (eV)	Ev (eV)	Ec (eV)
Furnace-treated undoped m-TiO_2 at 500 ºC	-4.37	3.04	3.37	-7.41	-4.04
Furnace-treated Li-doped m-TiO_2 at 500 ºC	-4.41	3.06	3.38	-7.47	-4.09
Laser-treated Li-doped m-TiO_2 at 800-850 ºC	-4.39	3.09	3.40	-7.48	-4.08

Table S5 The ratio of shoulder peak area to main peak area of O 1s peak with furnace-treated undoped m-TiO_2, Li-doped m-TiO_2 and laser-treated Li-doped m-TiO_2.

Conditions	Ratio (Shoulder Peak Area/ Main Peak Area)
Furnace-treated undoped m-TiO_2	0.26
Furnace-treated Li-doped m-TiO_2	0.34
Laser-treated Li-doped m-TiO_2	0.29

Table S6 Calculated parameters and trap density (N_t) for furnace-treated undoped m-TiO_2, Li-doped m-TiO_2 and laser-treated Li-doped m-TiO_2.

Samples	L (nm)	ε_r	V_{TFL} (V)	N_t (cm^{-3})
Furnace-treated undoped m-TiO_2	150	55	0.70	$1.89*10^{17}$
Furnace-treated Li-doped m-TiO_2	150	55	0.65	$1.76*10^{17}$
Laser-treated Li-doped m-TiO_2	150	55	0.58	$1.57*10^{17}$

Table S7 TRPL parameters for the perovskite films deposited on the different ETLs.

Conditions	τ_1(ns)	A_1 (%)	τ_2(ns)	A_2 (%)	τ_{avg}(ns)
Furnace-treated undoped TiO_2 at 500 ºC	51.34	18.71	247.91	81.29	238.97
Furnace-treated Li-doped m-TiO_2 at 500 ºC	50.42	14.27	174.23	85.73	168.54
Laser-treated Li-doped m-TiO_2 at 800-850 ºC	31.79	18.75	168.29	81.25	162.59

Table S8 Resistance of the ITO electrodes (covered by m-TiO_2) annealed with furnace and laser treatments.

Conditions	Resistance(Ω)
Before Laser treatment	151.42 ± 15.36
Furnace-treated at 500 ºC	721.78 ± 11.29
Laser-treated at 700-750 ºC	410.25 ± 13.65
Laser-treated at 800-850 ºC	435.63 ± 16.41
Laser-treated at 900-950 ºC	491.88 ± 17.52

Table S9 EIS fitting parameters for the devices with furnace-treated undoped TiO_2, Li-doped m-TiO_2 at 500ºC and laser treated Li-doped m-TiO_2 (800-850 ºC).

Conditions	R_s (Ω)	R_{rec} (Ω)	*CPE* (F)
Furnace-treated undoped TiO_2 at 500 ºC	47.6	1383.0	2.5e-8
Furnace-treated Li-doped m-TiO_2 at 500 ºC	44.8	1542.0	3.2e-8
Laser-treated Li-doped m-TiO_2 at 800-850 ºC	40.4	3477.0	2.8e-8

Table S10 Summary of photovoltaic parameters for the $Cs_{0.1}FA_{0.9}PbI_3$ devices with the furnace- and laser-treated Li-doped m-TiO_2 films.

Conditions	V_{OC} (V)	J_{SC} (mA·cm^{-2})	FF (%)	Average PCE (%)	Champion PCE (%)
Furnace-treated at 500 ºC	1.027±0.008	23.34±0.15	74.03±1.33	17.74±0.31	18.10
Laser-treated at 700-750 ºC	1.023±0.006	23.28±0.13	74.01±1.14	17.62±0.30	18.03
Laser-treated at 800-850 ºC	1.038±0.014	23.42±0.18	76.08±1.83	18.48±0.40	19.15
Laser-treated at 900-950 ºC	1.027±0.008	23.40±0.18	74.91±1.47	18.00±0.40	19.05

Table S11 Comparison of laser processing and conditional furnace processing.

Doping process	Processing temperature	Fabrication Conditions	Processing time (TiO_2 + doping process)	Performance of PSCs
Laser process (Li)	700-900℃	Ambient (this work)	21s + 21s	19.15%
Furnace process (Li)	450-500℃	Ambient (this work)	1.5h + 1.5h	18.10%
Flame annealing (Co)[16]	1000℃	Glove box	0.5h + 40s	19.6%
Furnace process (Li) [17]	450-500℃	Glove box	1.5h + 1.5h	17.59%
Furnace process (Nb) [18]	500℃	Glove box	0.5h +1.5h	13.4%
Hot plate (Nd) [19]	450-600℃	Glove box	0.75h + 3h	18.1%
Furnace process (Zn) [20]	450-500℃	Glove box	Unmentioned + 0.5h	18.3%

Table S12 The hysteresis index for the PSCs with the furnace-treated undoped m-TiO_2, furnace- and laser-treated Li-doped m-TiO_2.

Conditions	HI
Furnace-treated undoped m-TiO_2 at 500 ºC	0.38± 0.02
Furnace-treated Li-doped m-TiO_2 at 500 ºC	0.31± 0.01
Laser-treated Li-doped m-TiO_2 at 700-750 ºC	0.35± 0.02
Laser-treated Li-doped m-TiO_2 at 800-850 ºC	0.28± 0.02
Laser-treated Li-doped m-TiO_2 at 900-950 ºC	0.30± 0.01

Reference

1 J. Jeong, M. Kim, J. Seo, H. Lu, P. Ahlawat, A. Mishra, Y. Yang, M. A. Hope, F. T. Eickemeyer, M. Kim, Y. J. Yoon, I. W. Choi, B. P. Darwich, S. J. Choi, Y. Jo, J. H. Lee, B. Walker, S. M. Zakeeruddin, L. Emsley, U. Rothlisberger, A. Hagfeldt, D. S. Kim, M. Grätzel and J. Y. Kim, *Nature*, 2021, **592**, 381–385.

2 T. Zhong, L. Shi, H. Hao, J. Dong, K. Tang, X. Xu, S. L. Hamukwaya, H. Liu and J. Xing, *ACS Sustain. Chem. Eng.*, 2021, **9**, 13010–13020.

3 M. Wang, H. Sun, L. Meng, M. Wang and L. Li, *Adv. Mater.*, 2022, 2200041.

4 D. Wang, Q. Chen, H. Mo, J. Jacobs, A. Thomas and Z. Liu, *Mater. Adv.*, 2020, **1**, 2057–2067.

5 X. Xu, C. Ma, Y. M. Xie, Y. Cheng, Y. Tian, M. Li, Y. Ma, C. S. Lee and S. W. Tsang, *J. Mater. Chem. A*, 2018, **6**, 7731–7740.

6 U. D. Menda, G. Ribeiro, D. Nunes, T. Calmeiro, H. Águas, E. Fortunato, R. Martins and M. J. Mendes, *Mater. Adv.*, 2021, **2**, 6344–6355.

7 J. Troughton, K. Hooper and T. M. Watson, *Nano Energy*, 2017, **39**, 60–68.

8 W. Zhang, Y. Li, X. Liu, D. Tang, X. Li and X. Yuan, *Chem. Eng. J.*, 2020, **379**, 122298.

9 K. Huang, H. Li, C. Zhang, Y. Gao, T. Liu, J. Zhang, Y. Gao, Y. Peng, L. Ding and J. Yang, *Sol. RRL*, , DOI:10.1002/solr.201800318.

10 K. Jung, K. Oh, D. H. Kim, J. W. Choi, K. C. Kim and M. J. Lee, *Nano Energy*, 2021, **89**, 106387.

11 J. H. Lee, K. Jung and M. J. Lee, *J. Alloys Compd.*, 2021, **879**, 160373.

12 J. Zhao, G. He, D. Yang, D. Guo, L. Yang, J. Chen and D. Ma, *Sustain. Energy Fuels*, 2021, **5**, 4268–4276.

13 R. Xia, X. X. Gao, Y. Zhang, N. Drigo, V. I. E. Queloz, F. F. Tirani, R. Scopelliti, Z.

Huang, X. Fang, S. Kinge, Z. Fei, C. Roldán-Carmona, M. K. Nazeeruddin and P. J. Dyson, *Adv. Mater.*, , DOI:10.1002/adma.202003801.

14 Z. Wang, J. Jin, Y. Zheng, X. Zhang, Z. Zhu, Y. Zhou, X. Cui, J. Li, M. Shang, X. Zhao, S. Liu and Q. Tai, *Adv. Energy Mater.*, 2021, **11**, 1–8.

15 W. T. Wang, J. Sharma, J. W. Chen, C. H. Kao, S. Y. Chen, C. H. Chen, Y. C. Feng and Y. Tai, *Nano Energy*, 2018, **49**, 109–116.

16 J. K. Kim, S. U. Chai, Y. Ji, B. Levy-Wendt, S. H. Kim, Y. Yi, T. F. Heinz, J. K. Nørskov, J. H. Park and X. Zheng, *Adv. Energy Mater.*, 2018, **8**, 1–7.

17 A. Peter Amalathas, L. Landová, B. Conrad and J. Holovský, *J. Phys. Chem. C*, 2019, **123**, 19376–19384.

18 D. H. Kim, G. S. Han, W. M. Seong, J. W. Lee, B. J. Kim, N. G. Park, K. S. Hong, S. Lee and H. S. Jung, *ChemSusChem*, 2015, **8**, 2392–2398.

19 B. Roose, K. C. Gödel, S. Pathak, A. Sadhanala, J. P. C. Baena, B. D. Wilts, H. J. Snaith, U. Wiesner, M. Grätzel, U. Steiner and A. Abate, *Adv. Energy Mater.*, 2016, **6**, 1–7.

20 M. C. Wu, S. H. Chan, K. M. Lee, S. H. Chen, M. H. Jao, Y. F. Chen and W. F. Su, *J. Mater. Chem. A*, 2018, **6**, 16920–16931.